


From Particle Currents to Tracer Diffusion: Universal Correlation Profiles in Single-File Dynamics

Aurélien Grabsch¹, Théotim Berlioz¹, Pierre Rizkallah,² Pierre Illien,² and Olivier Bénichou¹

¹*Sorbonne Université, CNRS, Laboratoire de Physique Théorique de la Matière Condensée (LPTMC),
4 Place Jussieu, 75005 Paris, France*

²*Sorbonne Université, CNRS, Physico-Chimie des Électrolytes et Nanosystèmes Interfaciaux (PHENIX),
4 Place Jussieu, 75005 Paris, France*

 (Received 23 June 2023; revised 19 September 2023; accepted 27 November 2023; published 18 January 2024)

Single-file transport refers to the motion of particles in a narrow channel, such that they cannot bypass each other. This constraint leads to strong correlations between the particles, described by correlation profiles, which measure the correlation between a generic observable and the density of particles at a given position and time. They have recently been shown to play a central role in single-file systems. Up to now, these correlations have only been determined for diffusive systems in the hydrodynamic limit. Here, we consider a model of reflecting point particles on the infinite line, with a general individual stochastic dynamics. We show that the correlation profiles take a simple universal form, at arbitrary time. We illustrate our approach by the study of the integrated current of particles through the origin, and apply our results to representative models such as Brownian particles, run-and-tumble particles and Lévy flights. We further emphasise the generality of our results by showing that they also apply beyond the 1D case, and to other observables.

DOI: [10.1103/PhysRevLett.132.037102](https://doi.org/10.1103/PhysRevLett.132.037102)

Introduction.—Single-file transport, where particles move in narrow channels with the constraint that they cannot bypass each other, has become a fundamental model for transport in confined systems [1–5]. Experimentally, this situation has been observed in various physical, chemical, or biological systems, such as zeolites, colloidal suspensions, or carbon nanotubes [3–6]. Theoretically, it is a central field of statistical physics, relevant both at equilibrium and out of equilibrium [7,8]. In this context, two key observables have received a notable attention: (i) the integrated current through the origin Q_t (defined as the number of particles that have crossed the origin from left to right, minus those from right to left, up to time t) [9–15], and (ii) the position X_t of a tracer [1,2,16–26], which can be monitored experimentally at various scales [3–5].

Because the order of the particles is conserved at all times, strong correlations between these observables and the density of particles $\rho(x, t)$ emerge. For instance, an increase of Q_t imposes a density at the right of the origin higher than average, and a lower on the left. A similar effect occurs with X_t : a large displacement of the tracer in a given direction involves the displacement of more and more particles in the same direction. This leads to a striking subdiffusive behavior $\langle X_t^2 \rangle \propto \sqrt{t}$ [16] in contrast with the regular diffusion $\langle X_t^2 \rangle \propto t$.

Despite their importance, the quantification of the coupling between Q_t or X_t and $\rho(x, t)$ remains a broadly open question. Recently, they have been characterized for the symmetric exclusion process, and other paradigmatic

models of single-file diffusion [24–26]. In addition to their clear physical relevance, these correlations have also acquired a technical importance since they have been shown to satisfy a closed equation for these systems [24–27]. However, these results are limited to (i) the case of diffusive systems (in which the individual particles have a diffusive motion), (ii) the long time behavior, and (iii) the specific case of X_t and Q_t .

Here, by considering a model of reflecting point particles on the infinite line, with an arbitrary individual stochastic dynamics, we overcome these limitations. We show that the correlation profiles take a simple universal form (with respect to the individual motion of the particles), at arbitrary time, and for a large class of observables (as defined below).

More precisely, we illustrate our approach by the study the integrated current of particles through the origin, and apply our results to representative processes that go beyond Brownian particles, such as (i) run-and-tumble particles, which are a key model to describe active transport [29,30] and (ii) Lévy flights, which is an emblematic model of superdiffusion [31]. We further emphasize the generality of our results by showing that they also apply beyond the 1D case, and to other observables.

Model.—We first consider N particles on the real line, with position $\{x_i(t)\}_{i=1,\dots,N}$ at time t . In a second step, we will take the thermodynamic limit $N \rightarrow \infty$. Initially, the N particles are independently picked from a density $\rho_0(x)$, normalized such that $\int \rho_0(x) dx = N$. Each particle has a

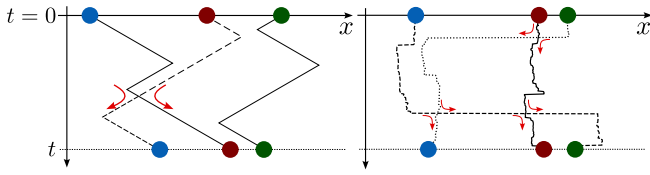


FIG. 1. The motion of reflective particles (illustrated by the arrows) can be mapped onto the motion of noninteracting particles (solid and dashed lines). Left: illustration with run-and-tumble particles, which move at a constant speed and flip their direction at random times. When two particles collide, they flip their direction. Right: Lévy flights. When a particle collides with another, it stops and the next particle is pushed. This can lead to a series of collisions.

stochastic dynamics in time, described by its propagator $G_t(x|y)$, i.e., the probability of finding the particle at position x at time t , knowing that it was at position y at time 0. When this dynamics leads to a crossing between two particles, they are simply exchanged, leading to a reflection of the particles. This dynamics can be mapped onto the one of *noninteracting* particles (see Fig. 1). While this formally applies to any propagator, this is especially relevant for Markovian dynamics, since the definition of the contact is more tricky in the non-Markovian case. The time evolution of the particles being independent from their initial distribution, we define two different types of averaging: (i) the average over the time evolution of the particles, denoted for any function f ,

$$\langle f(\{x_i(t)\}) \rangle = \int \prod_{i=1}^N dx_n K_t(\{x_i\}|\{x_i(0)\}) f(\{x_i\}), \quad (1)$$

with K_t the N -particles propagator, and (ii) the average over the initial positions,

$$\overline{f(\{x_i(0)\})} = \int \prod_{n=1}^N dy_n \frac{\rho_0(y_n)}{N} f(\{y_i\}). \quad (2)$$

Although our approach can be applied to many observables, we will focus for concreteness on the integrated current through the origin, which measures the variation of the number of particles on the positive axis,

$$Q_t = \sum_i \{\Theta[x_i(t)] - \Theta[x_i(0)]\}, \quad (3)$$

where Θ is the Heaviside step function. We are interested in the statistical properties of this observable, and its correlations with the global density of particles

$$\rho(x, t) = \sum_i \delta[x - x_i(t)]. \quad (4)$$

These two quantities are indeed expected to be strongly correlated. These correlations are encoded in the joint

cumulant generating function $\ln \langle e^{\lambda Q_t + \chi \rho(x,t)} \rangle$, where λ and χ are the parameters of the generating function. We have used here the *annealed* averaging, as usually defined in statistical mechanics, which corresponds to averaging over both the time evolution and all the initial positions. For simplicity, we will focus on the lowest orders in χ , which are the cumulant generating function of the integrated current, $\psi_A(\lambda, t) \equiv \lim_{N \rightarrow \infty} \ln \langle e^{\lambda Q_t} \rangle$, and the correlation profile [24]

$$w_A(x, \lambda, t) \equiv \lim_{N \rightarrow \infty} \frac{\langle \rho(x, t) e^{\lambda Q_t} \rangle}{\langle e^{\lambda Q_t} \rangle}. \quad (5)$$

These correlation profiles have been shown to play an important role, since they verify simple closed equations for several important models of single-file systems [24–26].

We also consider the case of a *quenched* initial condition, which corresponds to averaging over the time evolution of the typical initial positions of the particles. The initial condition is well-known to play a key role in single-file systems, as exemplified by “everlasting” effects on various observables [19,20,32–34]. In this case, the joint cumulant generating function is $\ln \langle e^{\lambda Q_t + \chi \rho(x,t)} \rangle$. At lowest orders in χ , this gives the quenched cumulant generating function $\psi_Q(\lambda, t) \equiv \lim_{N \rightarrow \infty} \overline{\ln \langle e^{\lambda Q_t} \rangle}$, and the quenched correlation profile

$$w_Q(x, \lambda, t) \equiv \lim_{N \rightarrow \infty} \frac{\overline{\langle \rho(x, t) e^{\lambda Q_t} \rangle}}{\overline{\langle e^{\lambda Q_t} \rangle}}. \quad (6)$$

Results.—The key ingredient is the joint propagator of the N particles, which takes the form [35]

$$K_t(\vec{x}|\vec{y}) = \frac{1}{N!} \sum_{\sigma} \prod_{i=1}^N G_t(x_i|y_{\sigma(i)}), \quad (7)$$

where the sum runs over all permutations σ of the N particles. Computing first the averages [(1), (2)] and then taking the thermodynamic limit $N \rightarrow \infty$ [36], we obtain that the cumulant generating function and the correlation profiles take a simple universal form (see Supplemental Material (SM) [37] for details of the derivation). In the annealed case,

$$\psi_A(\lambda, t) = \int dy \rho_0(y) \int [\tilde{G}_t^{(\lambda)}(x|y) - G_t(x|y)] dx, \quad (8)$$

$$w_A(x, \lambda, t) = \int \rho_0(y) \tilde{G}_t^{(\lambda)}(x|y) dy, \quad (9)$$

where we have defined the tilted propagator

$$\tilde{G}_t^{(\lambda)}(x|y) = e^{\lambda \Theta(x)} G_t(x|y) e^{-\lambda \Theta(y)}. \quad (10)$$

Similarly, in the quenched case,

$$\psi_Q(\lambda, t) = \int dy \rho_0(y) \ln \left[\int_{-\infty}^{\infty} \tilde{G}_t^{(\lambda)}(x|y) dx \right], \quad (11)$$

$$w_Q(x, \lambda, t) = \int dy \rho_0(y) \frac{\tilde{G}_t^{(\lambda)}(x|y)}{\int_{-\infty}^{\infty} \tilde{G}_t^{(\lambda)}(z|y) dz}. \quad (12)$$

These expressions hold for any propagator G_t of an individual particle, for any initial density of particles ρ_0 , and at arbitrary time t . They constitute the main results of this Letter. Note that our results hold in presence of external forces (a situation studied for instance in [38]) [39]. The key point of our derivation is that all the particles have the same dynamics (with the requirement that the memory of the past is lost upon collision), and feel the presence of the other particles only when a collision occurs. The only ingredient needed is the one particle propagator G_t , either analytically or numerically [40]. We now give the example of run-and-tumble particles, for which the propagator is known explicitly. This will allow us to discuss a concrete example of the physics of these correlation profiles. Formulas for the cases of Brownian particles and Lévy flights are given in SM [37].

Application: Run-and-tumble particles.—We consider a system of run-and-tumble particles, which is an important model of active particles, involved in various contexts [29,30]. These particles move at constant speed v_0 , and flip their direction of motion with rate γ . When two particles collide, they are reflected (see Fig. 1). For simplicity, we will consider a step initial density of particles $\rho_0(x) = \rho_+ \Theta(x) + \rho_- \Theta(-x)$. The Laplace transform of the propagator of an individual particle takes a simple form [29]. We can easily obtain the annealed profile and cumulant generating function in the Laplace domain since the expressions (8) and (9) are linear in the propagator. The inverse Laplace transform can be computed explicitly using the expressions given in [12], and we get $\psi_A(\lambda, t) = (\omega/2)v_0 t e^{-\gamma t} [I_0(\gamma t) + I_1(\gamma t)]$, where we have denoted $\omega = \rho_+(e^{-\lambda} - 1) + \rho_-(e^{\lambda} - 1)$, by analogy with the single parameter identified in the simple exclusion process [9], and I_ν is a modified Bessel function. Similarly, the correlation profile reads

$$w_A(x > 0, \lambda, t) = \rho_+ + \frac{\rho_- e^{\lambda} - \rho_+}{2} \Theta(v_0 t - x) \times \left(e^{-\frac{\gamma x}{v_0}} + \frac{\gamma x}{v_0} \int_1^{\frac{v_0 t}{x}} \frac{e^{-\frac{\gamma x T}{v_0}} I_1\left(\frac{\gamma x}{v_0} \sqrt{T^2 - 1}\right)}{\sqrt{T^2 - 1}} dT \right). \quad (13)$$

This profile, represented in Fig. 2, quantifies the correlation between the observable Q_t and the density of particles $\rho(x, t)$. When $\lambda > 0$, $w_A(x > 0, \lambda, t) \geq \rho_+$, indicating that

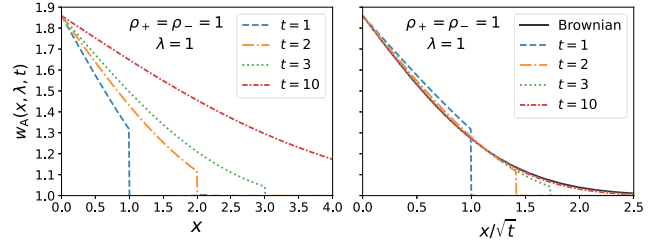


FIG. 2. Annealed correlation profile w_A (13) for run-and-tumble particles, with $v_0 = 1$ and $\gamma = 1$. Left: profile as a function of x for different times. Right: profile as a function of the rescaled variable x/\sqrt{t} at different times. For $t \rightarrow \infty$, it converges to the profile for diffusive particles (solid black lines), with a diffusion constant $D = v_0^2/(2\gamma) = \frac{1}{2}$.

an increase of the current yields an increase of the density at the right of the origin. We emphasise that (i) our approach captures the full dynamics of the profile w_A (13), illustrated in Fig. 2. In particular it presents a sharp cutoff at $x = v_0 t$, which is a consequence of the finite speed v_0 of the particles, showing that Q_t and $\rho(x, t)$ are decorrelated for $x > v_0 t$. (ii) The dependence of the profile (13) in ρ_+ , ρ_- and λ is in fact a general feature that holds for any propagator G_t , and is only a consequence of the choice of the observable Q_t and the initial step of density $\rho_0(x)$.

We now demonstrate that our approach can be extended in several important directions (see SM [37] for details).

Extension: Other geometry.—Our approach can be extended beyond the one-dimensional case, in particular to any tree geometry. An important example that has generated many works is the comb lattice [41–43]. Comb structures have been developed to represent diffusion in critical percolation clusters, with the backbone and teeth of the comb mimicking the quasilinear structure and the dead ends of percolation clusters [44]. More recently, the comb model has been used to account for transport in real systems such as spiny dendrites [45], diffusion of cold atoms [46], and diffusion in crowded media [47]. It is a two-dimensional lattice in which all the links parallel to the x axis have been removed, except those on the axis itself, called the backbone (see the inset in Fig. 3). The propagator of a particle performing a random walk on this lattice is given in [42]. In the continuous limit, the results [(8), (9), (11), and (12)] straightforwardly extend to this case, and leads to the correlation profile $w_A(\vec{r}, \lambda, t)$ shown in Fig. 3. It presents a different scaling with time in the two directions x and y , because particles can diffuse in the teeth of the comb, but horizontal motion is slowed down because it is only possible at $y = 0$.

Extension: Other observables.—The above discussion can be extended to observables of the form

$$\mathcal{O}_t[f, g] = \sum_i \{f[x_i(t)] - g[x_i(0)]\}, \quad (14)$$

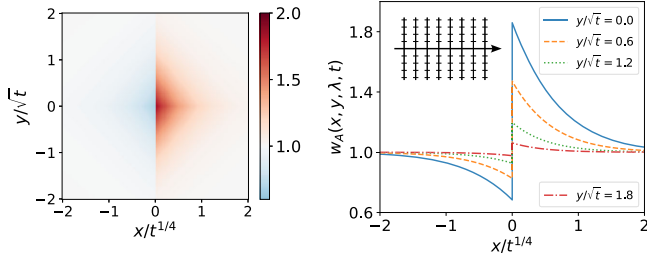


FIG. 3. Correlation profile $w_A[\vec{r} = (x, y), \lambda, t]$ for random walkers on a comb lattice in the annealed case (represented on the right plot), in the continuous limit. Left: 2D representation. The profile is a scaling function of $x/t^{1/4}$ and y/\sqrt{t} . Right: profile as a function of x for fixed values of y .

where f and g are two given functions, with $f(x) \underset{x \rightarrow \pm\infty}{\simeq} g(x)$ to ensure convergence of the sum. The case of the integrated current Q_t corresponds to $f = g = \Theta$. In general, the above results [(8), (9), (11), and (12)] still hold, but with the tilted propagator

$$\tilde{G}_t^{(\lambda)}(x|y) = e^{\lambda f(x)} G_t(x|y) e^{-\lambda g(y)}. \quad (15)$$

This provides in particular the profiles in the case of a generalized current $J_t(X)$, defined by $f(x) = \Theta(x - X)$ and $g(x) = \Theta(x)$. This observable measures the difference between the number of particles at the right of X at time t with the number of particles on the positive axis at $t = 0$. It has proved to be especially relevant since it can be used to find the position X_t of a tracer particle [48,49], given by $J_t(X_t) = 0$, meaning that no particle can cross the tracer. However, this only provides the final position X_t , and not the displacement $X_t - X_0$ (X_0 being the position of the first particle to the right of the origin, which is random).

Extension: Tracer particle.—Nevertheless, our method can be adapted to directly study the displacement of a tracer (placed initially at the origin for simplicity). So far, the only available studies concern the distribution of the tracer only [35,50], and not its correlations with the other particles, which are our main focus here. Extending the ideas of [1,20,35,50,51], the correlation profiles can be computed by noticing that the tracer can be mapped onto the “middle” particle of the system of noninteracting particles introduced above.

We now consider a finite system of $2N + 1$ particles, with initially N particles on the negative axis [positions $x_{-n}(t)$], N particles on the positive axis [positions $x_n(t)$], and a tracer initially at the origin [$x_0(t)$]. We define the average over the initial positions as

$$\overline{f(\{x_i(0)\})} = \int_{-\infty}^0 \prod_{n=1}^N \frac{\rho_0(y_{-n}) dy_{-n}}{N} \int_0^{\infty} \prod_{n=1}^N \frac{\rho_0(y_n) dy_n}{N} f(y_{-N}, \dots, y_{-1}, y_0 = 0, y_1, \dots, y_N). \quad (16)$$

The average over the time evolution is still given by (1). The probability of finding the tracer at position X at time t , with initially the particles at positions $\{x_i(0)\}$ can be obtained by imposing that there are still N particles to the left of the tracer, and N to the right,

$$P_t(X|\{x_i(0)\}) \equiv \langle \delta(X - x_0(t)) \rangle \propto \int_{-\infty}^X \prod_{n=1}^N dx_{-n} \times \int_X^{\infty} \prod_{n=1}^N dx_n K_t(\{x_n\}|_{x_0=X}|\{x_i(0)\}). \quad (17)$$

Using the expression of the joint propagator (7), and averaging over the time evolution and the initial positions (assumed to be annealed for simplicity), we obtain the distribution of $x_0(t)$ in the thermodynamic limit,

$$P_t(X) \equiv \lim_{N \rightarrow \infty} \overline{\langle \delta[X - x_0(t)] \rangle} = \int_{-\pi}^{\pi} f_t(X, \theta) e^{\phi_t(X, \theta)} d\theta, \quad (18)$$

where the integration over θ enforces the noncrossing constraint. The functions f_t and ϕ_t are expressed in terms of the propagator G_t (assumed translationally invariant and symmetric), its integral $F_t(z) = \int_z^{\infty} G_t(x|0) dx$, and the initial density of particles ρ_0 . The exact expressions are given in SM [37]. The distribution (18) extends to the out-of-equilibrium case of an arbitrary initial density ρ_0 , such as a step initial condition, the result of [50] obtained in the equilibrium case of a constant density. Here, we obtain in addition the full spatial dependence of the correlations between the position of the tracer and the density of surrounding particles, which takes the following simple and universal form:

$$\begin{aligned} \tilde{w}_A(x, X, t) &\equiv \lim_{N \rightarrow \infty} \frac{\overline{\langle \rho(x, t) \delta[X - x_0(t)] \rangle}}{\overline{\langle \delta[X - x_0(t)] \rangle}} \\ &= \alpha_t^{\pm}(X) G_t(x|0) + \beta_t^{\pm}(X) \rho_{\mp} F_t(\pm x) \\ &\quad + \rho_{\pm} F_t(\mp x), \end{aligned} \quad (19)$$

where the superscript \pm stands for $x \gtrless X$, with α_t^{\pm} and β_t^{\pm} given explicitly in SM [37]. We stress that the spatial dependence of these profiles is fully encoded in the propagator G_t (and its integral F_t). Note that we have considered in Eq. (19) here conditional profiles, which measure the mean density of particles conditioned on having observed the tracer at X at time t . In contrast, we have previously considered correlation profiles $\overline{\langle \rho(x, t) e^{\lambda x_0(t)} \rangle} / \overline{\langle e^{\lambda x_0(t)} \rangle}$. The two formulations are equivalent in the limit $t \rightarrow \infty$ [25,37], but not at arbitrary time. It turns out that the correlation profiles are more convenient to study observables of the form (14), while the conditional profiles are more suited to study tracer particles, since they

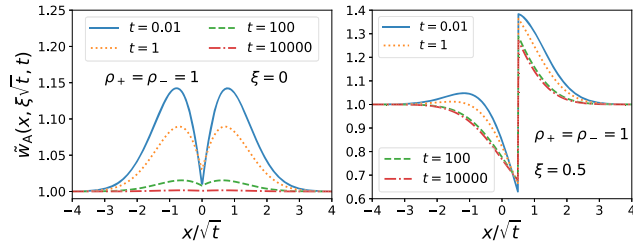


FIG. 4. Conditional density profiles \tilde{w}_A , for reflecting Brownian particles with diffusion coefficient $D = \frac{1}{2}$, with a tracer at position $X = \xi\sqrt{t}$, at different times t . Left: case $\xi = 0$, corresponding to a tracer conditioned to be at its mean position. Right: $\xi = 0.5$.

take a simple form. These conditional profiles are shown in Fig. 4 for reflective Brownian particles. At long times, they reach their asymptotic values computed in [24], but at arbitrary times they have a more complex structure, mostly due to the presence of the tracer at the origin at $t = 0$ [first term in (19)].

Extension: Two tracers.—Our approach can be extended to the important and largely unexplored situation of two tracers of positions $X_1(t)$ and $X_2(t)$. The only available studies in single-file systems concern the symmetric exclusion process and its limits [52–55], and the distance between two different particles at different times [56], which does not give access to the joint position of two tracers at the same time. We still obtain a simple form for the density profile conditioned on observing the first tracer at X and the second tracer at Y . As a byproduct, we obtain the strikingly simple, universal, and to the best of our knowledge new expression for the covariance of the displacements of two tracers,

$$\frac{\text{Cov}(X_1, X_2)}{\sqrt{\text{Var}(X_1)\text{Var}(X_2)}} \underset{t \rightarrow \infty}{\simeq} \frac{\int_z^\infty dx \int_x^\infty dy g(y)}{\int_0^\infty dx \int_x^\infty dy g(y)}, \quad (20)$$

where $z = [X_1(0) - X_2(0)]/\sigma_t$, and σ_t the long time scaling of the propagator $G_t(x|y) = g[(x - y)/\sigma_t]/\sigma_t$.

Conclusion.—We have shown that the correlation profiles in single-file systems take the strikingly simple universal form [(9)–(12)]. The approach is general and applies to (i) a broad range of dynamics (including with external forces or non-Markovian dynamics provided that the memory is lost upon collision); (ii) arbitrary time (note that these results are not accessible via the classical macroscopic fluctuation theory [57], which is limited to the large time behavior of diffusive systems [58]); (iii) different initial conditions (annealed and quenched [59]); (iv) various observables [the form (14) includes the joint statistics of several currents [37]]; and (v) geometries not restricted to the single-file constraint (illustrated by the comb geometry). In addition, beyond the clear physical relevance of the correlation profiles, the simplicity of (9)–(12) further highlights their key role to describe transport properties in confined geometry [13–15, 18, 24–26, 28, 48, 49].

- [1] D. G. Levitt, *Phys. Rev. A* **8**, 3050 (1973).
- [2] R. Arratia, *Ann. Probab.* **11**, 362 (1983), <https://www.jstor.org/stable/2243693>.
- [3] K. Hahn, J. Kärger, and V. Kukla, *Phys. Rev. Lett.* **76**, 2762 (1996).
- [4] Q.-H. Wei, C. Bechinger, and P. Leiderer, *Science* **287**, 625 (2000).
- [5] B. Lin, M. Meron, B. Cui, S. A. Rice, and H. Diamant, *Phys. Rev. Lett.* **94**, 216001 (2005).
- [6] S. Cambré, B. Schoeters, S. Luyckx, E. Goovaerts, and W. Wenseleers, *Phys. Rev. Lett.* **104**, 207401 (2010).
- [7] P. L. Krapivsky, S. Redner, and E. Ben-Naim, *A Kinetic View of Statistical Physics* (Cambridge University Press, Cambridge, 2010).
- [8] T. Chou, K. Mallick, and R. K. Zia, *Rep. Prog. Phys.* **74**, 116601 (2011).
- [9] B. Derrida and A. Gerschenfeld, *J. Stat. Phys.* **136**, 1 (2009).
- [10] B. Derrida and A. Gerschenfeld, *J. Stat. Phys.* **137**, 978 (2009).
- [11] P. L. Krapivsky and B. Meerson, *Phys. Rev. E* **86**, 031106 (2012).
- [12] T. Banerjee, S. N. Majumdar, A. Rosso, and G. Schehr, *Phys. Rev. E* **101**, 052101 (2020).
- [13] K. Mallick, H. Moriya, and T. Sasamoto, *Phys. Rev. Lett.* **129**, 040601 (2022).
- [14] E. Bettelheim, N. R. Smith, and B. Meerson, *Phys. Rev. Lett.* **128**, 130602 (2022).
- [15] D. S. Dean, S. N. Majumdar, and G. Schehr, *arXiv:2303.08961*.
- [16] T. E. Harris, *J. Appl. Probab.* **2**, 323 (1965).
- [17] A. Ryabov and P. Chvosta, *J. Chem. Phys.* **136**, 064114 (2012).
- [18] P. L. Krapivsky, K. Mallick, and T. Sadhu, *Phys. Rev. Lett.* **113**, 078101 (2014).
- [19] P. L. Krapivsky, K. Mallick, and T. Sadhu, *J. Stat. Mech.* (2015) P09007.
- [20] T. Sadhu and B. Derrida, *J. Stat. Mech.* (2015) P09008.
- [21] J. Cividini, A. Kundu, S. N. Majumdar, and D. Mukamel, *J. Stat. Mech.* (2016) 053212.
- [22] J. Cividini, A. Kundu, S. N. Majumdar, and D. Mukamel, *J. Phys. A* **49**, 085002 (2016).
- [23] A. Kundu and J. Cividini, *Europhys. Lett.* **115**, 54003 (2016).
- [24] A. Poncet, A. Grabsch, P. Illien, and O. Bénichou, *Phys. Rev. Lett.* **127**, 220601 (2021).
- [25] A. Grabsch, A. Poncet, P. Rizkallah, P. Illien, and O. Bénichou, *Sci. Adv.* **8**, eabm5043 (2022).
- [26] A. Grabsch, P. Rizkallah, A. Poncet, P. Illien, and O. Bénichou, *Phys. Rev. E* **107**, 044131 (2023).
- [27] Note that, since the publication of [25] in which this closed equation first appears, the exactness of the equation has been proved [13] using the inverse scattering method (see also [14, 28]).
- [28] A. Krajenbrink and P. Le Doussal, *Phys. Rev. E* **107**, 014137 (2023).
- [29] G. H. Weiss, *Physica (Amsterdam)* **311A**, 381 (2002).
- [30] J. Tailleur and M. E. Cates, *Phys. Rev. Lett.* **100**, 218103 (2008).
- [31] J.-P. Bouchaud and A. Georges, *Phys. Rep.* **195**, 127 (1990).
- [32] N. Leibovich and E. Barkai, *Phys. Rev. E* **88**, 032107 (2013).

- [33] A. Poncet, O. Bénichou, and P. Illien, *Phys. Rev. E* **103**, L040103 (2021).
- [34] J. Krug, H. Kallabis, S. N. Majumdar, S. J. Cornell, A. J. Bray, and C. Sire, *Phys. Rev. E* **56**, 2702 (1997).
- [35] C. Rödenbeck, J. Kärger, and K. Hahn, *Phys. Rev. E* **57**, 4382 (1998).
- [36] We have introduced the initial density of particles ρ_0 with the constraint that it is normalized to N . In the thermodynamic limit $N \rightarrow \infty$, this constraint relaxes and one can consider non-normalized initial densities, such as $\rho_0(x) = \rho$ constant.
- [37] See Supplemental Material at <http://link.aps.org/supplemental/10.1103/PhysRevLett.132.037102> for details.
- [38] A. P. Antonov, A. Ryabov, and P. Maass, *Phys. Rev. Lett.* **129**, 080601 (2022).
- [39] Note that our results hold in the presence of external forces, but not for arbitrary interparticle interactions, since this latter case involves the full many-body propagator that cannot be reduced to a single-particle propagator in the general case.
- [40] If the propagator is known analytically, our main results (8)–(12) yield explicit expressions for the cumulants and profiles. If the propagator is obtained numerically, our results provide a straightforward way to compute these observables numerically by at most two numerical integrations.
- [41] O. Bénichou, P. Illien, G. Oshanin, A. Sarracino, and R. Voituriez, *Phys. Rev. Lett.* **115**, 220601 (2015).
- [42] P. Illien and O. Bénichou, *J. Phys. A* **49**, 265001 (2016).
- [43] A. Iomin, V. Méndez, and W. Horsthemke, *Fractional Dynamics in Comb-Like Structures* (World Scientific, Singapore, 2018).
- [44] G. H. Weiss and S. Havlin, *Physica (Amsterdam)* **134A**, 474 (1986).
- [45] V. Méndez and A. Iomin, *Chaos Solitons Fractals* **53**, 46 (2013).
- [46] Y. Sagi, M. Brook, I. Almog, and N. Davidson, *Phys. Rev. Lett.* **108**, 093002 (2012).
- [47] F. Höfling and T. Franosch, *Rep. Prog. Phys.* **76**, 046602 (2013).
- [48] T. Imamura, K. Mallick, and T. Sasamoto, *Phys. Rev. Lett.* **118**, 160601 (2017).
- [49] T. Imamura, K. Mallick, and T. Sasamoto, *Commun. Math. Phys.* **384**, 1409 (2021).
- [50] C. Hegde, S. Sabhapandit, and A. Dhar, *Phys. Rev. Lett.* **113**, 120601 (2014).
- [51] P. L. Krapivsky, K. Mallick, and T. Sadhu, *J. Stat. Phys.* **160**, 885 (2015).
- [52] S. Majumdar and M. Barma, *Physica (Amsterdam)* **177A**, 366 (1991).
- [53] O. Takeshi, S. Goto, T. Matsumoto, A. Nakahara, and M. Otsuki, *Phys. Rev. E* **88**, 062108 (2013).
- [54] T. Ooshida and M. Otsuki, *J. Phys. Condens. Matter* **30**, 374001 (2018).
- [55] A. Poncet, O. Bénichou, V. Démerly, and G. Oshanin, *Phys. Rev. E* **97**, 062119 (2018).
- [56] S. Sabhapandit and A. Dhar, *J. Stat. Mech.* (2015) P07024.
- [57] L. Bertini, A. De Sole, D. Gabrielli, G. Jona-Lasinio, and C. Landim, *Rev. Mod. Phys.* **87**, 593 (2015).
- [58] For diffusive systems, the macroscopic fluctuation theory gives access to correlation profiles of the form $\langle \rho(x, \tau T) e^{\lambda O_\tau} \rangle / \langle e^{\lambda O_\tau} \rangle$ with T large and $0 \leq \tau \leq 1$. Here, we have obtained correlation profiles of the form $\langle \rho(x, t) e^{\lambda O_t} \rangle / \langle e^{\lambda O_t} \rangle$ for arbitrary t .
- [59] The quenched case is notoriously more difficult than the annealed case: for instance while the annealed cumulant generating function of the current in the symmetric exclusion process has been determined in [9], its quenched counterpart is still missing.